J Mater Sci: Mater Electron (2015) 26:6887–6891
DOI 10.1007/s10854-015-3305-8

Synthesis, structures and properties of single phase $BiFeO_3$ and $Bi_2Fe_4O_9$ powders by hydrothermal method

Bin Hu[1] · Jin-Feng Wang[1] · Ji Zhang[1] · Zheng-Bin Gu[1] · Shan-Tao Zhang[1]

Received: 12 March 2015 / Accepted: 1 June 2015 / Published online: 6 June 2015

Abstract Single phase $BiFeO_3$ and $Bi_2Fe_4O_9$ powders have been synthesized via hydrothermal method by carefully controlling the reaction conditions. It is found that the $BiFeO_3$ shows dense microstructure with irregular, larger grains, the average grain size is $\sim$5.0 μm, whereas the $Bi_2Fe_4O_9$ displays small, porous microstructure with the sheet shaped grains, the average thickness is $\sim$55 nm and length is $\sim$500 nm. X-ray photoemission spectra confirm that in both compositions, the Bi and Fe cations have the charge valence of +3. The magnetization–magnetic field (M–H) and magnetization–temperature (M–T) measurements reveal that the $BiFeO_3$ has weak ferromagnetism even at room temperature due to its canted antiferromagnetic interaction, whereas the $Bi_2Fe_4O_9$ shows antiferromagnetic nature in the temperature range of 10–300 K. Our results provide interesting supplements for controlling the morphology and understanding the structure–property relationship of $BiFeO_3$ and $Bi_2Fe_4O_9$.

1 Introduction

Multiferroics materials with at least two coexisted ferroic orders have attracted much attention due to their possible applications in novel devices like multiple-state memories and data-storage media as well as their fascinating fundamental physics like unique and strong coupling between magnetic, electric, and structural order parameters. $BiFeO_3$ is one of the most outstanding multiferroic materials with coexisted ferroelectric (Curie temperature $T_c \sim 1103$ K) and antiferromagnetic (Néel temperature $T_N \sim 643$ K) orders. $BiFeO_3$ has been investigated in many forms [1–3]. On the other hand, $Bi_2Fe_4O_9$ is generally easy to be formed as the second phase during the process of preparing $BiFeO_3$ powder or ceramics, making the phase purity of $BiFeO_3$ to be very processing-sensitive [4]. Actually, $Bi_2Fe_4O_9$ is also an excellent multiferroic material with ferroelectric ($T_c \sim 250$ K) and antiferromagnetic ($T_N \sim 260$ K) [5], but there are relatively less reports focusing on this material [5–7]. Though single-phase $BiFeO_3$ and $Bi_2Fe_4O_9$ are obtainable independently, their condition windows for fabricating are still critical and narrow, so it still remains a challenge to prepare single phase $BiFeO_3$ and $Bi_2Fe_4O_9$ easily. On the other hand, it is well known that $BiFeO_3$ has special magnetic structure, which makes the magnetic property is size-sensitive [1–3]. Based on these descriptions, further works are still necessary to study the relationship between preparing conditions and phase purity, morphologies, properties, etc. For this aim, it is necessary to prepare both materials using the same method so as to comparatively investigate their preparation condition, structures, and properties, etc.

Up to now, solid state reaction and many wet chemical methods, such as molten salt method, sol–gel, and co-precipitation, were used to prepare $BiFeO_3$ and $Bi_2Fe_4O_9$ powders. As well known, compared with other methods, the hydrothermal reaction route is a very important synthetic method to prepare metal-oxide materials with its advantages of low-cost, simple process and well-controllable processing [8–10].

Accordingly, in this paper we report a facial hydrothermal process for synthesizing single phase $BiFeO_3$

✉ Shan-Tao Zhang
stzhang@nju.edu.cn

[1] National Laboratory of Solid State Microstructures and Department of Materials Science and Engineering, College of Engineering and Applied Science, Nanjing University, Nanjing 210093, China

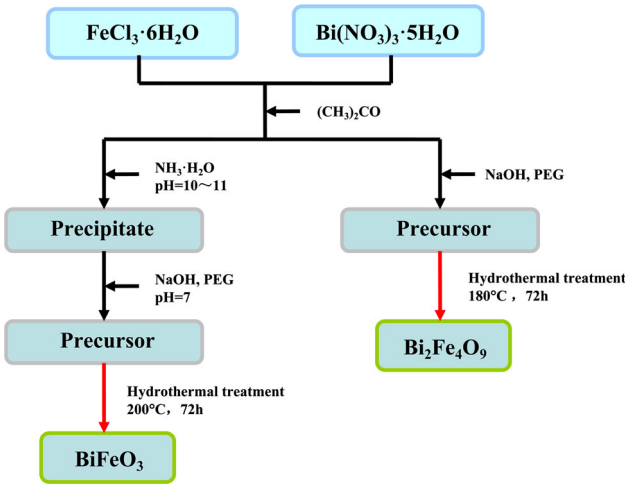

Fig. 1 The detailed preparation flowchart for the $BiFeO_3$ and $Bi_2Fe_4O_9$ powders

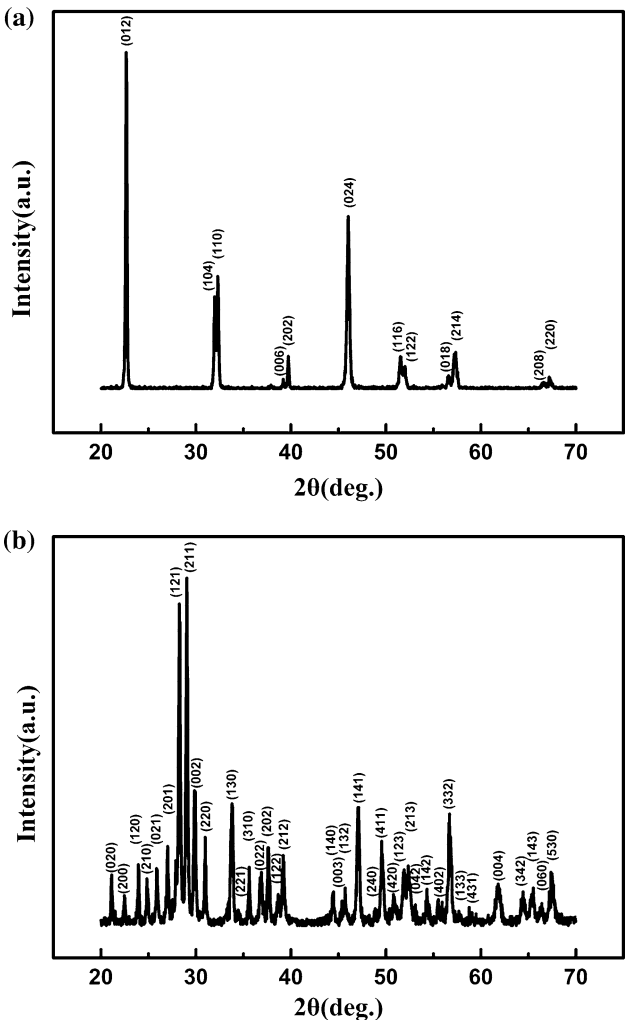

Fig. 2 XRD patterns of the **a** $BiFeO_3$ and **b** $Bi_2Fe_4O_9$ powders

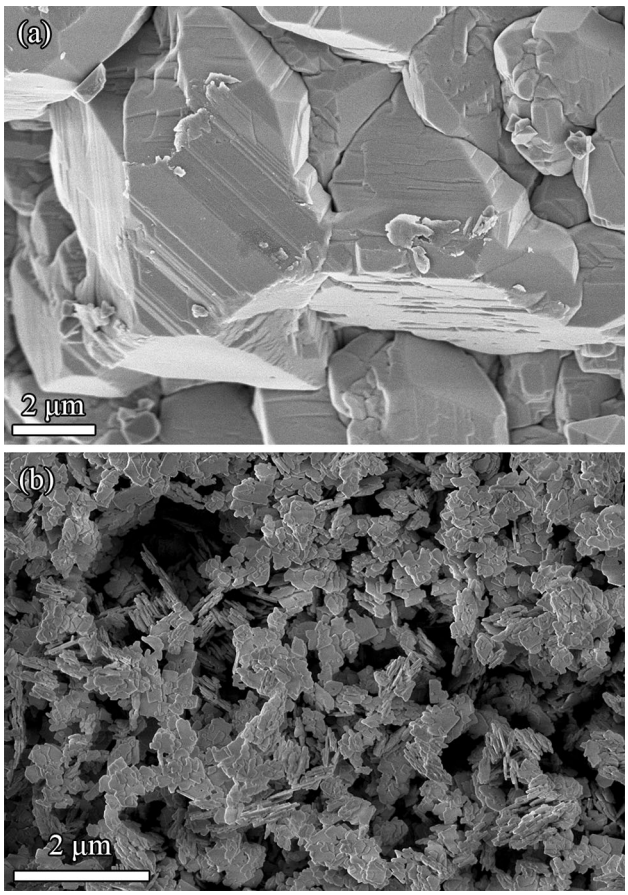

Fig. 3 SEM micrograph of the **a** $BiFeO_3$ and **b** $Bi_2Fe_4O_9$ powders

and $Bi_2Fe_4O_9$ powders. Their phase purity, morphology, cation's charge valence, and magnetic property were comparatively investigated.

2 Experimental procedure

The $BiFeO_3$ and $Bi_2Fe_4O_9$ samples were synthesized by hydrothermal method, detailed preparation flowchart is presented in Fig. 1. All the chemicals used are analytic grade reagents without further purification. Iron chloride hexahydrate ($FeCl_3{\cdot}6H_2O$) and bismuth nitrate [$Bi(NO_3)_3{\cdot}5H_2O$] were used as the source materials, sodium hydroxide (NaOH) were added as a mineralizer, while polyethylene glycol (PEG) as additives. Deionized water was used to make all aqueous solutions. In the typical procedure of the $BiFeO_3$ powder, 5 mmol $Bi(NO_3)_3{\cdot}5H_2O$ and 5 mmol $FeCl_3{\cdot}6H_2O$ (1:1 in molar ratios) were dissolved in 50 ml acetone with stirring and ultrasound until completely dissolved. Then, 200 ml deionized water were added and the pH value of the above solution was controlled to be

10–11 by adding concentrated ammonia. The sediment was centrifuged out and washed with deionized water several times till the pH value was 7. Subsequently, 8 g NaOH and 40 ml deionized water were added with stirring for 30 min. The solution was transferred to a Teflon-lined stainless-steel autoclave and heated at 200 °C for 72 h, and then cooled to room temperature (RT) in air naturally. The products were filtered and washed several times with deionized water and absolute ethanol, and finally dried in air at 70 °C for 24 h. As for the preparation of $Bi_2Fe_4O_9$, 5 mmol $Bi(NO_3)_3{\cdot}5H_2O$ and 5 mmol $FeCl_3{\cdot}6H_2O$ in a stoichiometric ratio, were dissolved in 50 ml acetone with stirring and ultrasound until completely dissolved. Then 3.2 g NaOH and 0.8 g PEG (Mw $= 4 \times 10^4$ g/mol) were added with stirring for 30 min. The solution was transferred to a 50 ml Teflon-lined stainless-steel autoclave and heated at 180 °C for 72 h, and then cooled to RT in air naturally. The products were filtered and washed several times with deionized water and absolute ethanol, and finally dried in air at 70 °C for 24 h.

The crystal structures of the powder were characterized by powder XRD (Rigaku Ultima III) with Cu-Kα radiation operated at 40 kV and 40 mA with a step size of 0.03°. The microstructures were analyzed by scanning electron microscopy (SEM, ULTRA55, Zeiss). The chemical states of the Bi and Fe cations in both $BiFeO_3$ and $Bi_2Fe_4O_9$ samples were analyzed by X-ray photoelectron spectroscopy (XPS, Thermo Fisher Scientific K-Alpha), which was performed at a base pressure of 5×10^{-7} mbar. Photoelectric peak of C1s located at 284.6 eV was used as the criterion to rectify binding energies of XPS spectra. The magnetization–magnetic field (M–H) curves and the zero-field-cooled (ZFC) and field-cooled (FC) magnetization–temperature (M–T) curves were measured by using a physical property measurement system (PPMS, Quantum Design).

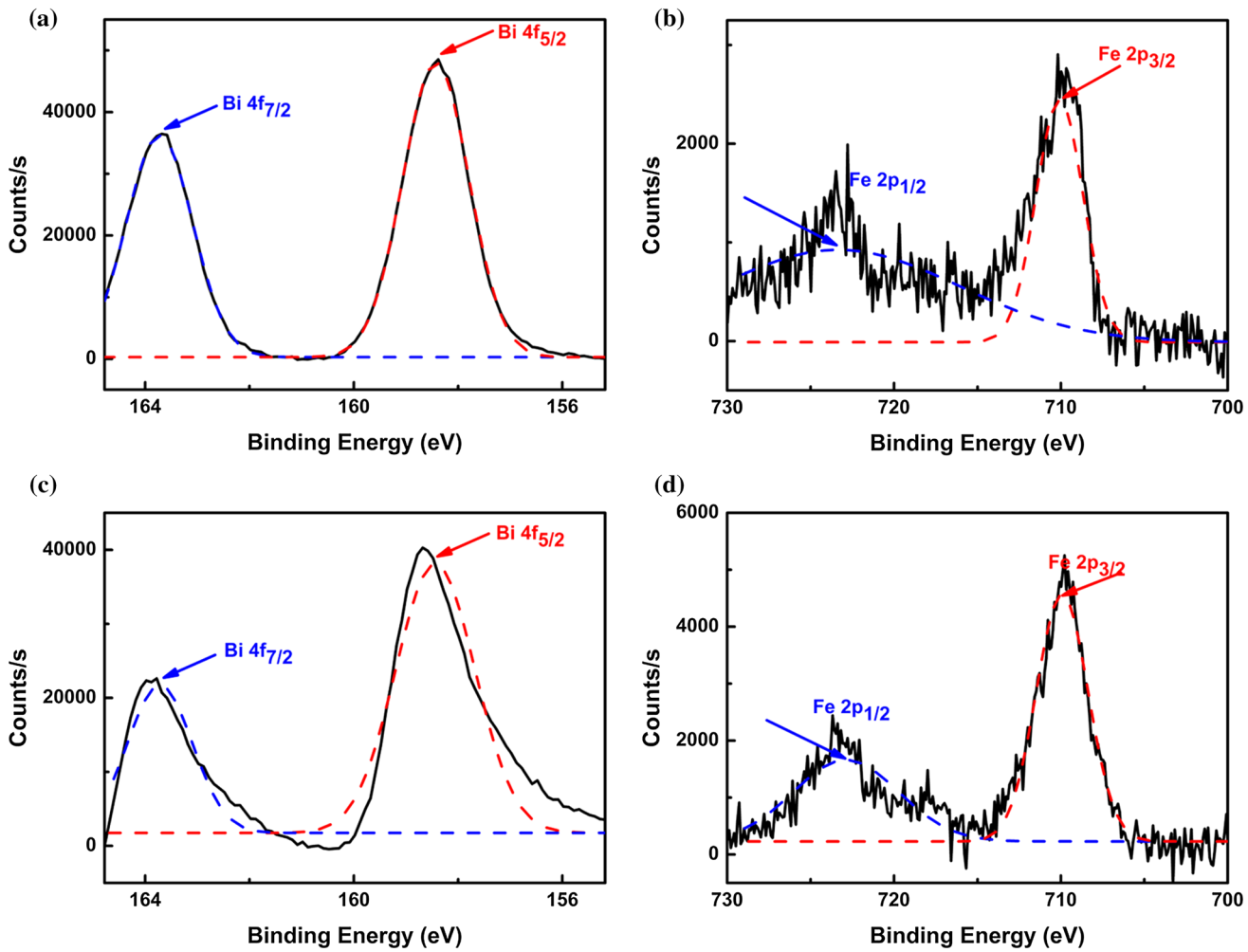

Fig. 4 XPS spectra of the Bi and Fe cations in (**a**, **b**) $BiFeO_3$ and **c**, **d** $Bi_2Fe_4O_9$

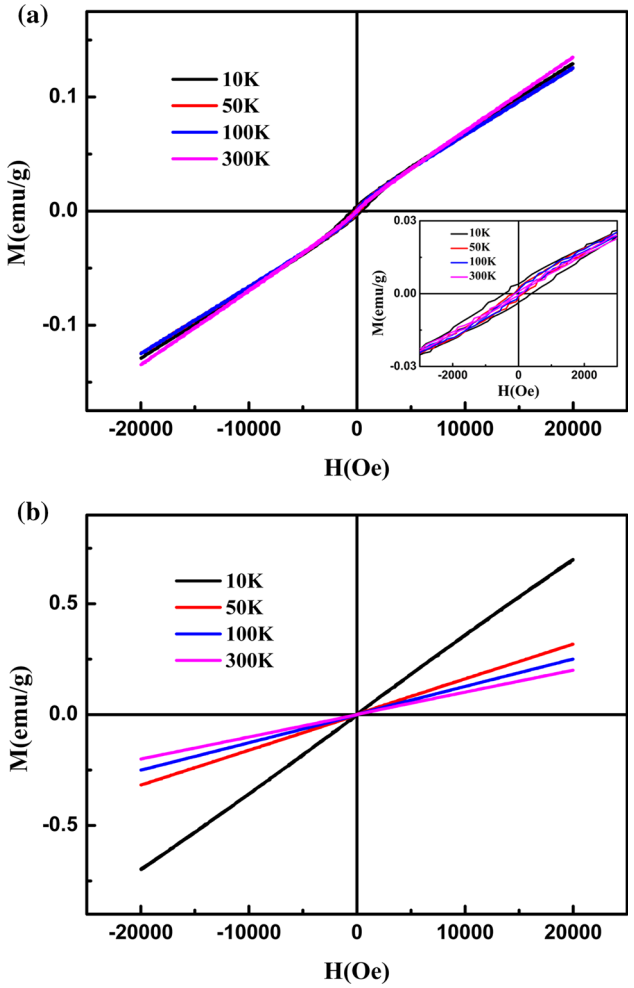

Fig. 5 M–H curves of **a** $BiFeO_3$ and **b** $Bi_2Fe_4O_9$ measured at 10, 50, 100, and 300 K. The *inset* of **a** shows the partly enlarged curves

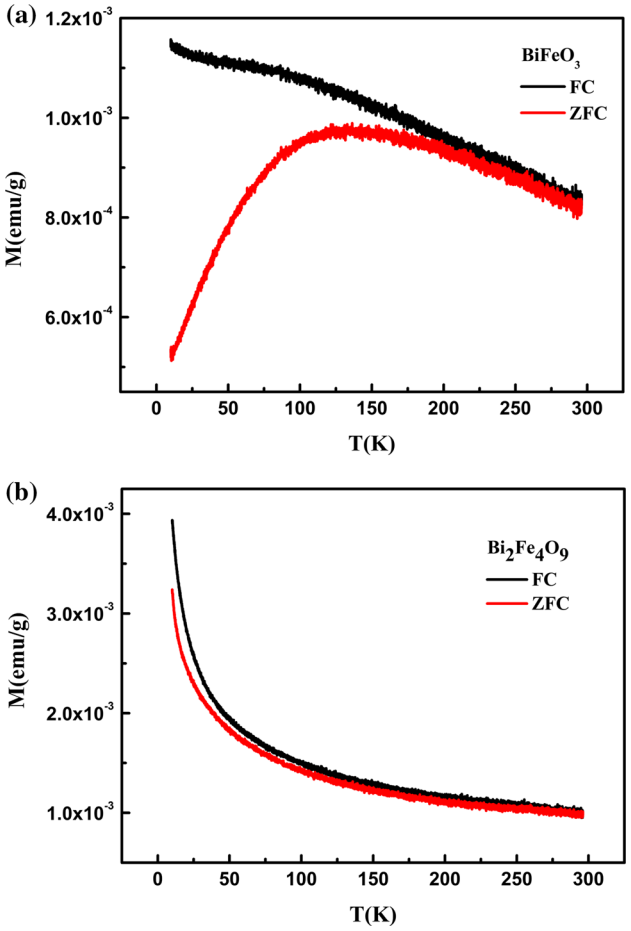

Fig. 6 M–T curves of **a** $BiFeO_3$ and **b** $Bi_2Fe_4O_9$

3 Results and discussion

Figure 2a, b shows the XRD patterns of the as-prepared $BiFeO_3$ and $Bi_2Fe_4O_9$ samples, respectively. In generally, the XRD patterns reveal that the as-prepared $BiFeO_3$ and $Bi_2Fe_4O_9$ samples are single-phase without detectable second phases [2, 5, 7–9]. The diffraction peaks in Fig. 2a can be assigned to the $BiFeO_3$ (JCPDS No. 20-0169), indicating the $BiFeO_3$ powder has rhombohedral perovskite structure (space group: *R3c*), as reviewed in Ref. [2]. On the other hand, the XRD patterns of $Bi_2Fe_4O_9$ samples can be indexed to the orthorhombic structure, which are consistent with the standard data (JCPDS No. 25-0090) and other reports [5, 7].

The micrographs of $BiFeO_3$ and $Bi_2Fe_4O_9$ are displayed in Fig. 3a, b, respectively. For the $BiFeO_3$ samples, dense microstructures with large, irregular grains are obtained, the average grain size is $\sim$5.0 μm. However, the $Bi_2Fe_4O_9$ has relatively smaller, porous microstructure with sheet shaped grains with the average size of $\sim$500 nm in length and $\sim$55 nm in thickness. Actually, $BiFeO_3$ is easy to from relatively uniform particles [7], whereas $Bi_2Fe_4O_9$ has the tendency to form sheet shaped microstructure [11]. As well known, $BiFeO_3$ has rhombohedral structure with lattice of $a = b = c \sim 5.6$ Å and $\alpha \sim 60°$, while $Bi_2Fe_4O_9$ has orthorhombic structure with $a \sim 7.9$ Å, $b \sim 8.4$ Å, $c \sim 5.9$ Å [7, 12]. Clearly $Bi_2Fe_4O_9$ has higher degree structural anisotropy than $BiFeO_3$, especially along *c*-axis direction, therefore, the growing rates may be different in different direction, leading to sheet-shaped morphology. However, this is not the case for $BiFeO_3$, thus relatively uniform grains are obtained.

The XPS was used to investigate the chemical states of Bi and Fe in both samples, typical results are shown in Fig. 4a, b, respectively. The XPS spectra show that the binding energies of Bi $4f_{5/2}$, Bi $4f_{7/2}$, Fe $2p_{1/2}$ and Fe $2p_{3/2}$ peaks in both samples are located at 158.5, 163.9, 724.3 and 711.5 eV, respectively, suggesting that Bi^{3+}, Fe^{3+} existed in the pure $BiFeO_3$ and $Bi_2Fe_4O_9$ samples [13]. No peak corresponding to Fe^{2+} can be detected. Furthermore, the XPS spectra also indicate that the $BiFeO_3$ and $Bi_2Fe_4O_9$

powders are a single phase, which is in good agreement with the XRD measurements shown in Fig. 2.

The M–H curves of the $BiFeO_3$ and $Bi_2Fe_4O_9$ have been measured at 10, 50, 100 and 300 K under a maximum field of 20 kOe, as presented in Fig. 5a, b, respectively. $BiFeO_3$ is known to be antiferromagnetic with a *G*-type magnetic structure but has a residual magnetic moment due to a canted spin structure, consistent with the weak hysteresis (the inset of Fig. 5a), therefore, it is reasonable that $BiFeO_3$ shows weak ferromagnetism in the whole temperature range (10–300 K). At 10 K and 20 kOe external field, the maximum magnetization and remnant magnetization are about 0.13 and 0.004 emu/g, respectively, consistent with other report [13, 14]. It is noted the magnetization is relatively lower than nano-sized $BiFeO_3$ [15], which is due to the size effect: small $BiFeO_3$ can suppress the spiral spin structure with period of $\sim$62 nm. $Bi_2Fe_4O_9$ has antiferromagnetic order, so it is responsible it shows almost linear M–H curves (Fig. 5b), the magnetization value at maximum field is consistent with other report [5]. For both samples, the magnetization decreases with increasing temperature due to their antiferromagnetic order.

In order to further investigate the magnetic properties of the $BiFeO_3$ and $Bi_2Fe_4O_9$, FC and ZFC magnetization–temperature (M–T) curves are measured, as shown in Fig. 6a, b. In Fig. 6a, a remarkable separation between the FC and ZFC is observed, one can see the ZFC curve, a cusp which corresponds to the freezing temperature ($T_f \sim 125$ K) is observed. Within a temperature range of 300 K to T_f, the ZFC and FC magnetization values nearly superpose and increase with the decreasing temperature, indicating that the $BiFeO_3$ is antimagnetic. The ZFC and FC curves of $BiFeO_3$ start to diverge when the temperature is close to $T_f = 125$ K. The divagation of ZFC and FC magnetizations at low temperatures and cusps (T_f) are typical characteristics of spin-glass behavior. These results are consistent with the phenomenon observed in Fig. 6a. For the sheet shaped $Bi_2Fe_4O_9$ sample, the magnetization in both ZFC and FC M–T curves show a rapid increase at low temperatures (Fig. 6b). This may be due to the spin-glass-like behavior caused by the nanoscaled particles, and is consistent with the antiferroelectric nature observed in Fig. 5b. The FC and ZFC curves tend to diverge around 250 K, in good agreement with the reported Neel temperature T_N.

4 Conclusion

In summary, single phase $BiFeO_3$ and $Bi_2Fe_4O_9$ are synthesized by hydrothermal method. With the same bismuth and iron sources, two kinds of bismuth ferrite compounds with different morphologies can be synthesized by carefully controlling the hydrothermal reaction conditions. Different morphologies are observed and attributed to the different crystal structures. In addition, $BiFeO_3$ shows weak ferromagnetic behavior at low temperature range whereas $Bi_2Fe_4O_9$ is antiferromagnetic in the whole measuring temperature range. Our results may be helpful for optimizing the preparation conditions and furthering understanding the structure–property relationship of $BiFeO_3$ and $Bi_2Fe_4O_9$.

Acknowledgments This work was supported by the National Nature Science Foundation of China (11174127).

References

1. J.G. Park, M.D. Le, J. Jeong, S. Lee, J. Phys. Condens. Matter **26**, 433202 (2014)
2. T. Rojac, A. Bencan, B. Malic, G. Tutuncu, J.L. Jones, J.E. Daniels, D. Damjanovic, J. Am. Ceram. Soc. **97**, 1993 (2014)
3. N. Nuraje, K. Su, Nanoscale **5**, 8752 (2013)
4. J. Chen, R.B. Yu, L.H. Li, C. Sun, T. Zhang, H.W. Chen, X.R. Xing, Eur. J. Inorg. Chem. **23**, 3655 (2008)
5. M. Liu, H.B. Yang, Y. Lin, Y. Yang, J. Mater. Sci. Mater. Electron. **25**, 4949 (2014)
6. C.M. Raghavan, J.W. Kim, J.Y. Choi, J.W. Kim, S.S. Kim, Ceram. Int. **40**, 14165 (2014)
7. X. Wang, M. Zhang, P. Tian, W.S. Chin, C.M. Zhang, Appl. Surf. Sci. **321**, 144 (2014)
8. N.I. IIic, A.S. Dzunuzovic, J.D. Bobic, B.S. Stojadinovic, P. Hammer, M.M.V. Petrovic, Z.D. Dohcevi-Mitrovic, B.D. Stojanovic, Ceram. Int. **41**, 69 (2015)
9. M. Ahmadzadeh, A. Ataie, E. Mostafavi, J. Alloys Compd. **622**, 548 (2015)
10. A. Saxena, P. Sharma, A. Saxena, V. Verma, R.S. Saxena, Ceram. Int. **40**, 15065 (2014)
11. H. Sun, Y. Liu, Y. Zhang, L. Lv, J. Zhou, W. Chen, J. Mater. Sci. Mater. Electron. **25**, 4212 (2014)
12. S.T. Zhang, M.H. Lu, D. Wu, Y.F. Chen, N.B. Ming, Appl. Phys. Lett. **87**, 262907 (2005)
13. Z. Chen, W. Jin, J. Mater. Sci. Mater. Electron. **25**, 4039 (2014)
14. G.L. Yuan, S.W. Or, J. Appl. Phys. **100**, 024109 (2006)
15. R. Köferstein, J. Alloys Compd. **590**, 324 (2014)